

# Self-Scaling of the Statistical Properties of a Minimal Model of the Atmospheric Circulation

Valerio Lucarini<sup>1,2</sup>, Antonio Speranza<sup>1</sup>, Renato Vitolo<sup>1</sup>

<sup>1</sup> University of Camerino, Department of Mathematics and Computer Science, Camerino, Italy, [lucarini@alum.mit.edu](mailto:lucarini@alum.mit.edu)

<sup>2</sup> University of Bologna, Department of Physics, Bologna, Italy

**Abstract.** A quasi-geostrophic intermediate complexity model of the mid-latitude atmospheric circulation is considered, featuring simplified baroclinic conversion and barotropic convergence processes. The model undergoes baroclinic forcing towards a given latitudinal temperature profile controlled by the forced equator-to-pole temperature difference  $T_E$ . As  $T_E$  increases, a transition takes place from a stationary regime - Hadley equilibrium - to a periodic regime, and eventually to a chaotic regime, where evolution takes place on a strange attractor. The dependence of the attractor dimension, metric entropy, and bounding box volume in phase space is studied by varying  $T_E$ . It is found that this dependence is smooth and has the form of a power-law scaling. The observed smooth dependence of the system's statistical properties on the external parameter  $T_E$  is coherent with the chaotic hypothesis proposed by Gallavotti and Cohen, which entails an effective structural stability for the attractor of the system. Power-law scalings with respect to  $T_E$  are also detected for global observables responding to global physical balances, like the total energy of the system and the averaged zonal wind. The scaling laws are conjectured to be associated with the statistical process of baroclinic adjustment, decreasing the equator-to-pole temperature difference. The observed self-similarity could be helpful in setting up a theory for the overall statistical properties of the general circulation of the atmosphere and in guiding - also on a heuristic basis - both data analysis and realistic simulations, going beyond the unsatisfactory mean field theories and brute force approaches.

## 1 Introduction

The problem of understanding climate is an issue of scientific as well as practical interest, since it is connected to aspects of vital importance for human life and environment. Recently, climate has also become a politically relevant issue. In this chapter we propose our scientific approach and some encouraging results concerning the theory of General Atmospheric Circulation (GAC) - the core machine of weather and climate - looked upon as a problem in Physics. Climate is defined as the set of the

statistical properties of the climatic system. In its most complete definition, the climatic system is composed of four intimately interconnected sub-systems, atmosphere, hydrosphere, cryosphere, and biosphere. These subsystems interact nonlinearly with each other on various time-space scales (Lucarini 2002). The atmosphere is the most rapid component of the climatic system, features both many degrees of freedom, which makes it complicated, and nonlinear interactions of different components involving a vast range of time scales, which makes it complex. The GAC is a realization of planetary scale thermodynamic transformations in a rotating, stratified fluid. Among all the physical processes involved in the GAC, the so-called baroclinic conversion plays a central role because it is through this mechanism that the available potential energy (Margules 1903; Lorenz 1955), stored in the form of thermal fluctuations, is converted into the vorticity and kinetic energy of the air flows. Apart from the classical role of baroclinic instability (Charney 1947; Eady 1949) in mid-latitude weather development (Dell'Aquila et al. 2005), different forms of baroclinic conversion operate at larger scales (*e.g.* in the ultra-long planetary waves associated with the so called low-frequency variability (Charney and DeVore 1979; Benzi et al. 1986; Benzi and Speranza 1989; Ruti et al. 2006), and at smaller scales (*e.g.* in the banded sub-frontal structures (Mantovani and Speranza 2002).

Historically - see the classical monograph by Lorenz (1967) - the problem of GAC has been essentially approached in terms of analyzing the time-mean circulation. Usual separations such as between time average and fluctuations or between the zonal and the eddy field, are somewhat arbitrary, but perfectly justifiable with arguments of symmetry, evaluation of statistical moments, etc.. The time average-fluctuations separation is often suggestive of a theory in which the fluctuations growing on an unstable basic state, identified with the time average, feed back onto the basic state itself and *stabilize* it. The central objective of the classical circulation theory is the *closure* in the form of a *parameterization* of the nonlinear eddy fluxes in terms of quantities which can be derived from the mean field itself. This approach is not only unsuccessful, it is just not feasible, because the stability properties of the time mean state do not provide even a zeroth-order approximation of the dynamical properties of the full nonlinear system. This has been illustrated by theoretical arguments (Farmer 1983) and counter-examples of physical significance (Speranza and Malguzzi 1988; Malguzzi et al. 1990). As a consequence, even sophisticated versions of the idea that the GAC dynamics may be defined in terms of the statistics derivable from average atmospheric fields have proved unfruitful for guiding the interpretation of observations and the development of models.

Alternative approaches have been proposed, *e.g.* mimicking the GAC via dynamical systems approach with simplified low-dimensional models, say below 10 degrees of freedom (Ghil et al. 1985). However, the physical relevance and mathematical generality of these approaches has been criticized as well, whereas the rele-

vance of the space-time geophysical scaling behavior has been emphasized (Scherzer and Lovejoy 2004). Nevertheless, a comprehensive and coherent picture of the GAC is still far from being available and the classical *time-mean* approach has not been completely abandoned as a paradigm.

It is clear that in the context of the classic paradigm of GAC, the main task of modeling consists in capturing the mean field: the fluctuations will follow as its instabilities. This point of view, whether explicit or not, has strongly influenced the set-up and diagnostics of existing General Circulation Models (GCMs). As a consequence, the diagnostic studies usually focus on comparing the temporal averages of the simulated fields rather than on analyzing the dynamical processes provided by the models. Similar issues are related to the provision of the so-called extended range weather forecasts. Suppose, in fact, that the forecaster was given the next month average atmospheric fields: what practical information could he derive from that? Of course, if dynamical information were stored in the average fields - typically in the form of dominant regimes of instability derivable from the stability analysis of time-mean flow - he could obtain useful information from the prediction of such time mean fields. Actually, the problem of extended range forecast is still open even in terms of clearly formulating what we should forecast in place of average fields.

Profound scientific difficulties arise when considering the GAC from a statistical mechanics point of view. In spite of several attempts (see *e.g.* Leith 1975), it is actually impossible to establish straightforward analogues of the fluctuation-dissipation theorem (Kubo 1966), or of Kramers-Kronig relations (Lucarini et al. 2005): a forced and dissipative chaotic system is rather different from a Hamiltonian system immersed in a thermal bath. It is therefore impossible to construct a Climate Change theory on this basis, essentially because the GAC features the non-equivalence between the external and internal fluctuations (Lorenz 1979). The main reason for this non-equivalence is that, because of dissipation, the attractor of the system lives on a manifold of zero volume inside its phase space: the internal *natural* fluctuations occur within such a manifold whereas externally induced fluctuations would move the system out of the attractor with probability 1. In other words, ergodicity does not hold in the whole phase space, as usually assumed in equilibrium statistical mechanics along the Boltzmann paradigm. In this case, ergodicity - if present at all - is restricted to the attractor, which is identified as a Sinai-Ruelle-Bowen (SRB) measure (Eckmann and Ruelle 1985). This concept lies at the basis of the Chaotic hypothesis formulated in a recent set of papers by Gallavotti and Cohen (1996; 1999). The project of *writing* sets of equations directly describing the statistics of the system on the attractor (the projection of the original equations of motion onto the attractor) has been carried on with great attention in the recent past (Lorenz 1980; Fritz and Robinson 2001). But, despite the big efforts, no applicable result has been obtained so far (Foias and Olson 1996).

In the absence of robust scientific paradigms, a gap was created between the studies revolving around phenomenological and/or numerical modeling issues and those focused on fundamental mechanisms of GAC (Held 2005). The assumption that adopting models of ever increasing resolution will eventually lead to the final understanding of the GAC (a sort of *brute force* approach) is not based on any consolidated mathematical and physical knowledge and may, in fact, result misleading. One basic reason is that, in the limit of infinite resolution for any numerical model of fluid flow, the numerical convergence to the statistical properties (infinite time) of the continuum real fluid flow dynamics is not guaranteed. As a matter of fact, we note that at the present stage, most of the leading climate models are neither consistent nor realistic even in the representation of the basic time-space spectral properties of the variability of the atmosphere at mid-latitudes (Lucarini et al. 2006).

Finally, problems arise when auditing climate models, since we have always to deal with three qualitatively distinct attractors: the attractor of the real atmosphere; the reconstruction of the real attractor from observations; the attractors of the model (maybe more than one) we adopt in climatic studies. The first one is obviously unknown; as for the second one, the (presumably) best reconstructions available are provided by the reanalyses (Kalnay 2003). Note that presently there are two alternative main global reanalyses, which, albeit generally in good agreement, disagree on some distinct statistical properties (Dell'Aquila et al. 2005; Ruti et al. 2006). As for the third kind of attractors, the various GCMs surely possess substantially different attractors, which reflects into disagreements in the statistical properties of the atmosphere (Lucarini et al. 2006).

This chapter wishes to give hints for addressing the following question: once we abandon the unsatisfactory mean field theories, what may come next? What may lead a new approach to a theory of GAC, which can serve as a guidance for setting up and diagnosing GCMs? Which statistical properties may be crucial? Therefore, we are, at this stage, not seeking realism in the model representation of atmospheric dynamics, but rather searching for representations of key nonlinear processes with the minimum of ingredients necessary to identify the properties under investigation. We have decided to choose a rather simplified quasi-geostrophic (QG) model with just a few hundreds degrees of freedom, able to capture the central processes of the mid-latitude portion of the GAC. In Sec. 2 we discuss the derivation of the evolution equations for the two-layer QG model. In Sec. 3 we characterize the transition from stationary to chaotic dynamics in terms of bifurcation theory and study the dependence on  $T_E$  and on model resolution  $JT$  of the dimension of the strange attractor, of the metric entropy, and of the volume of its bounding box in the phase space. In Sec. 4 we analyze the statistics of two physically meaningful observables, namely the total energy of the system and the latitudinally averaged zonal wind. In Sec. 5 we give our conclusive remarks and perspectives for future works.

## 2 The Model

The description of the large scale behavior of the atmosphere is usually based on the systematic use of dominant balances, which are derived on a phenomenological diagnostic basis, but whose full-correctness at theoretical level is still unclear. When considering the dynamics of the atmosphere at mid-latitudes, on spatial and temporal scales comparable with or larger than those of the synoptic weather (about 1000 Km and 1 day, respectively), the hydrostatic and geostrophic balances are phenomenologically well-established. From the set of *ab-initio* dynamic and thermodynamic equations of the atmosphere it is possible to obtain a set of simplified prognostic equations for the synoptic weather atmospheric fields in a domain centered at mid-latitudes - the QG equations - by assuming that the fluid obeys the hydrostatic balance and undergoes small departures from the geostrophic balance (Charney 1948; Pedlosky 1987; Speranza and Lucarini 2005). A great number of physical phenomena are *filtered out* of the equations by the QG approximation: various types of waves associated with strong local divergence, turbulent motions, etc.. There is no doubt that these are small on the time-space scales of the motions we consider, but it is still an open question to what extent they influence or not the statistics of large scale atmospheric motions and, in case, how to model such a statistical effect. Note that in general the QG attractor is not a good approximation to the attractor of the corresponding full *ab-initio* equations, despite the fact that the QG balance approximation is diagnostically quite good for the dominating time-space scales of the atmosphere (Lorenz 1980).

In this work we consider a  $\beta$ -channel periodic domain, with  $x \in R / 2\pi L$  denoting the zonal and  $y \in [0, L_y]$  the latitudinal coordinate. As a further approximation, we consider only two vertical layers (Phillips 1954). This is the minimal system retaining the baroclinic conversion process, which is the basic physical feature of the QG approximation. In order to avoid problems in the definition of the boundary conditions of the model, due to the prescription of the interaction with the polar and the equatorial circulations at the northern and southern boundary, respectively (Speranza and Malguzzi 1988), we consider a domain extending from the pole to the equator. Near the equator the QG approximation is not valid, so that the representation of the actual tropical circulation is beyond the scope. The equations of motions are:

$$D_t^1(\Delta_H \psi_1 + f_0 + \beta y) - f_0 \frac{\omega_2 - \omega_0}{\delta p} = 0, \quad (1)$$

$$D_t^3(\Delta_H \psi_3 + f_0 + \beta y) - f_0 \frac{\omega_4 - \omega_2}{\delta p} = 0, \quad (2)$$

$$D_t^2 \left( \frac{\psi_1 - \psi_3}{\delta p} \right) - H^2 \frac{f_0}{p_2^2} \omega_2 = \kappa \Delta_H \left( \frac{\psi_1 - \psi_3}{\delta p} \right) + \frac{R}{p_2 f_0} \frac{Q_2}{C_p}. \quad (3)$$

where  $f_0$  is the Coriolis parameter and  $\beta$  its meridional derivative evaluated at the center of the channel,  $\kappa$  parameterizes the heat diffusion,  $R$  and  $C_p$  are the thermodynamical constants for dry air,  $\Delta_H$  is the horizontal laplacian operator. Moreover, the streamfunction  $\psi_j$  is defined at pressure levels  $p = p_{j=1} = p_0/4$  and  $p = p_{j=3} = 3/4 p_0$ , while the vertical velocity  $\omega$  is defined at the pressure levels  $p = p_{j=0} = 0$  (top boundary),  $p = p_{j=2} = p_0/2$ , and  $p = p_{j=4} = p_0$  (surface boundary). The pressure level pertaining to the discrete approximation to vertical derivative of the streamfunction  $\partial \psi_j / \partial p$  as well as the stratification height  $H$  is  $p = p_{j=2}$ , and  $\delta p = p_3 - p_1 = p_2 = p_0/2$ .  $Q_2$  is the diabatic heating, and  $D_t^j$  is the usual Lagrangian derivative defined at the pressure level  $p_j$ ,  $D_t^j \bullet = \partial_t + J(\psi_j, \bullet)$ , where  $J$  is the conventional Jacobian operator defined as  $J(A, B) = \partial_x A \partial_y B - \partial_y A \partial_x B$ . The streamfunction at the intermediate level  $p_2$  is computed as average between the streamfunctions of the levels  $p_1$  and  $p_3$ , so that the material derivative at the level  $p_2$  can be expressed as  $D_t^2 = 1/2(D_t^1 + D_t^3)$ . We choose the following simple functional form for the diabatic heating:

$$Q_2 = \nu_N C_p (T^* - T_2) = \nu_N C_p \frac{f_0 p_2}{R} \left( \frac{2\tau^*}{\delta p} - \frac{\psi_1 - \psi_3}{\delta p} \right), \quad (4)$$

where the temperature  $T_2$  is evaluated at the pressure level 2 and is defined via hydrostatic relation, which implies that the system is relaxed towards a prescribed temperature profile  $T^*$  with a characteristic time scale of  $1/\nu_N$ .  $T^*$  and  $\tau^*$  are respectively defined as follows:

$$T^* = \frac{T_E}{2} \cos\left(\frac{\pi y}{L_y}\right), \quad \tau^* = \frac{R}{f_0} \frac{T_E}{4} \cos\left(\frac{\pi y}{L_y}\right), \quad (5)$$

so that  $T_E$  is the forced temperature difference between the low and the high latitude border of the domain. In our simulations we assume no time dependence for the forcing parameter  $T_E$ , thus discarding the seasonal effects. Since by thermal wind relation  $(\bar{u}_1 - \bar{u}_3) / \delta p = \hat{k} \times \bar{\nabla} / (\psi_1 - \psi_3) / \delta p$ , we have that the diabatic forcing  $Q_2$  in causes a relaxation of the vertical gradient of the zonal wind  $u_1 - u_3$  towards the prescribed profile  $2m^* = 2d\tau^*/dy$ , where the constant 2 has been introduced for later convenience.

By imposing  $\omega_0 = 0$  (top of the atmosphere) and assuming  $\omega_4 = -E_0 \Delta_H \psi_3$  - Ekman pumping (Pedlosky 1987) - and after a rearrangement of Eqs. (1)-(3), one obtains the evolution equations for the baroclinic field  $\tau = 1/2(\psi_1 - \psi_3)$  and the barotropic field  $\phi = 1/2(\psi_1 + \psi_3)$ :

$$\partial_t \Delta_H \tau - \frac{2}{H_2^2} \partial_t \tau + J \left( \tau, \Delta_H \phi + \beta y + \frac{2}{H_2^2} \phi \right) + J(\phi, \Delta_H \tau) = \frac{2\nu_E}{H_2^2} \Delta_H (\phi - \tau) - \frac{2\kappa}{H_2^2} \Delta_H \tau + \frac{2\nu_N}{H_2^2} (\tau - \tau^*), \quad (6)$$

$$\partial_t \Delta_H \phi + J(\phi, \Delta_H \phi + \beta y) + J(\tau, \Delta_H \tau) = -\frac{2\nu_E}{H_2^2} \Delta_H (\phi - \tau). \quad (7)$$

where  $\nu_E = f_0 E_0 H_2^2 / (2\delta p)$  is the viscous-like coupling between the free atmosphere and the planetary boundary layer via Ekman pumping, and the meaning of  $\tau^*$  is made clear. Notice that this system only features quadratic nonlinearities.

Variable	Scaling Factor	Value of the scaling factor
$x, y$	1	$10^6 m$
$t$	$u^{-1} l$	$10^5 s$
$\psi_1, \psi_3, \phi, \tau$	ul	$10^7 m^2 s^{-1}$
$U, m$	u	$10 ms^{-1}$
$\lambda_1, \dots, \lambda_{6JT}$	$ul^{-1}$	$10^{-5} s^{-1}$
$t_p$	$u^{-1} l$	$10^5 s$
$T$	$ul f_0 R^{-1}$	$3.5 K$
$E$	$u^2 l^2$	$5.1 \times 10^{17} J$

**Tab. 1.** Variables of the system and their scaling factors.

The two-layer QG system can be brought to the non-dimensional form, which is more usual in the meteorological literature and is easily implementable in computer codes. This is achieved by introducing length and velocity scales  $l$  and  $u$  and performing a non-dimensionalization of both the system variables  $(x, y, t, \phi, \tau, T)$  (as described in Tab. 1) and of the system constants (Tab. 2); in our case appropriate values are  $l = 10m^6$  and  $u = 10ms^{-1}$ .

In this work we consider a simplified spectral version of Eqs. (6)-(7), where truncation is performed in the zonal Fourier components so that only the zonally symmetric component and one of the non-symmetric components are retained. The derivation is reported in Speranza and Malguzzi (1988). The main reason for this choice is that we wish to focus on the interaction between the zonal wind and waves, thus neglecting the wave-wave nonlinear interactions. Since quadratic nonlinearities generate terms with Fourier components corresponding to the sum and difference of the Fourier components of the two factors, we can exclude direct wave-wave interactions provided that we only retain a single wave component (see, *e.g.*, Lucarini et al. (2005) for a general discussion of these effects in a different context). Note that if cubic nonlinearities were present, direct self wave-wave interaction would have been

possible (Malguzzi and Speranza 1981; Benzi et al 1986). In the present case, the wave can self-interact only indirectly through the changes in the values of the zonally symmetric fields. This amounts to building up equations which are *almost-linear*, in the sense that the wave dynamics is linear with respect to the zonally symmetric parts of the fields (*i.e.*, the winds). The wavelength of the only retained wave component is  $L_x/6$ , since we intend to represent the baroclinic conversion processes, which in the real atmosphere take place on scales of  $L_x/6$  or smaller (Dell'Aquila et al. 2005). In so doing we are retaining only one of the classical ingredients of GAC, *i.e.* the *zonal wind-wave* interaction.

Parameter	Dimensional Value	Non-dimensional value	Scaling factor
$L_x$	$2.9 \times 10^7 m$	29	1
$L_y$	$10^7 m$	10	1
$H_2$	$7.07 \times 10^5 m$	$7.07 \times 10^{-1}$	1
$f_0$	$10^{-4} s^{-1}$	10	$ul^{-1}$
$\beta$	$1.6 \times 10^{-11} m^{-1} s^{-1}$	1.6	$ul^2$
$v_E$	$5.5 \times 10^5 m^2 s^{-1}$	$5.5 \times 10^{-2}$	$ul$
$v_N$	$1.1 \times 10^{-6} s^{-1}$	$1.1 \times 10^{-1}$	$ul^{-1}$
$\kappa$	$2.75 \times 10 m^2 s^{-1}$	$2.75 \times 10^{-1}$	$ul$
$T_E$	28 K to 385 K	8 to 110	$ul f_0 R^{-1}$

**Tab. 2.** Parameters of the system and their scaling factors. The system is equivalent to what presented in Malguzzi and Speranza (1988) with the following correspondences:

Both  $\phi$  and  $\tau$  are thus determined by 3 real fields: the zonally symmetric parts and the real and imaginary part of the only retained zonal Fourier component. A pseudospectral decomposition with  $JT$  modes is then applied to the resulting 6 real fields in the  $y$ -direction, yielding a set of  $6 \times JT$  ordinary differential equations in the spectral coefficients. For the truncation order  $JT$  we have used the values  $JT = 8, 16, 32, 64$ . This is the prototypal model we use as *laboratory* for the analysis of the GAC. The only form of realism we are trying to achieve here is that the statistical properties of the nonlinear cycle *baroclinic instability - barotropic & baroclinic stabilization* are represented.

### 3 Dynamical and statistical characterization of the model attractor

The system of equations (6)-(7) has a stationary solution describing a zonally symmetric circulation, characterized by the stationary balance between the horizontal temperature gradient and the vertical wind shear. This solution corresponds on the Earth system to the idealized pattern of the Hadley equilibrium (Held and Hou



1980). There is a value of the equator-to-pole temperature gradient  $T_E^H$  such that if  $T_E < T_E^H$  the Hadley equilibrium is stable and has a virtually infinite basin of attraction, whereas if  $T_E > T_E^H$  it is unstable.

In the stable regime with  $T_E < T_E^H$ , after the decay of transients, the fields  $\phi$ ,  $\tau$ , and  $T$  are time-independent and feature zonal symmetry - they only depend on the variable  $y$ . Moreover, they are proportional by the same near-to-unity factor to the corresponding relaxation profiles. In particular, this implies that all the equilibrium fields are proportional to the parameter  $T_E$ .

JT	$T_E^H$	$T_E^{crit}$
8	7.83	9.15
16	8.08	8.42
32	8.28	8.52
64	8.51	8.66

**Tab. 3.** Values of  $T_E$  such that the Hadley equilibrium loses stability via Hopf bifurcation ( $T_E^H$ ) and where the onset of the chaotic regime occurs ( $T_E^{crit}$ ).

When increasing the values of the control parameter  $T_E$  beyond  $T_E^H$ , the equilibrium becomes unstable - as first pointed out on vertically continuous models (Charney 1947; Eady 1949) and on the two two-layer model (Phillips 1954) - with respect to the process of baroclinic conversion. This allows for the transfer of available potential energy of the zonal flow stored into the meridional temperature gradient into energy of the eddies, essentially transferring energy from the latter component to the first two components of the energy density expression, later presented in Eq. (10). The observed value of  $T_E^H$  increases with the considered truncation order  $JT$  (see Tab. 3). A finer resolution allows for more efficient stabilizing mechanisms, because they act preferentially on the small scales. Such mechanisms are the barotropic stabilization of the jet, increasing the horizontal shear through the convergence of zonal momentum, which is proportional to the quadrature of the spatial derivatives of the fields  $\phi$  and  $\tau$  (Kuo 1973), and the viscous dissipation, which is proportional to the Laplacian of the fields  $\phi$  and  $\tau$ . This is a clarifying example that, in principle, it is necessary to include suitable renormalizations in the parameters of a model when changing the resolution  $JT$ , in order to keep correspondence with the resulting dynamics (Lorenz 1980). In our case the values of  $T_E^H$  obtained for the adopted resolutions are rather similar. A stable periodic orbit branches off from the Hadley equilibrium as  $T_E$  increases above  $T_E^H$ . The attracting periodic orbit persists for  $T_E$  in a narrow interval, where it disappears through a saddle-node bifurcation taking place on an attracting invariant two-torus. For slightly larger values of  $T_E$ , *i.e.* for  $T_E > T_E^{crit}$ , a strange attractor develops by so-called quasi-periodic breakdown of a

*doubled* torus. This is one of the most typical routes for onset of chaos (weak turbulence) in fluid dynamics experiments and low-dimensional models, compare (Broer et al. 2002; Randriamampianina et al. 2005) and references therein. The invariant objects involved in the transition to low-dynamical chaos correspond to well-known fluid flow patterns. In particular, the two-torus attractor in phase space yields an *amplitude vacillation* in the flow (Randriamampianina et al. 2005). For  $JT = 8$ , a different route to chaos takes place, involving a quasi-periodic Hopf bifurcation of the two-torus (instead of a quasi-periodic period doubling), whereby an invariant three-torus is created. The question remains open whether the signature of the bifurcations of the system, of the kind exploited in the context of physical oceanography in a recent book (Dijkstra 2005), is present in the geometrical structure of the fully developed strange attractor and is potentially useful for computing the statistical properties.

### 3.1 Lyapunov Exponents and Dimension of the Strange Attractor

To characterize the dynamical properties of the strange attractors of the truncated system we study of the Lyapunov exponents (Oseledec 1968; Eckmann and Ruelle 1985), which are denoted, as customary, by  $\lambda_1, \lambda_2, \dots, \lambda_N$ , with  $\lambda_1 \geq \lambda_2 \geq \dots \geq \lambda_N$ ,  $N = 6 \times JT$ . The maximal exponent  $\lambda_1$  becomes positive as  $T_E$  crosses the torus breakdown value  $T_E^{crit}$ , and then increases monotonically with  $T_E$ . Despite the schematic approach adopted in this work, the obtained Lyapunov spectra are qualitatively similar to what reported in Vannitsem (1997) and Snyder and Hamill (2003), where a much larger number of degrees of freedom was considered. The distribution of the exponents approaches a smooth shape for large  $T_E$ , which suggests the existence of a well-defined *infinite baroclinicity* model obtained from as a (possibly, singular perturbation) limit for  $T_E \rightarrow \infty$ . We will analyze elsewhere this mathematical property, which is possibly of physical interest as well.

The Lyapunov exponents are used to compute the Lyapunov dimension (also called Kaplan-Yorke dimension, see Eckmann and Ruelle (1985) and Kaplan and Yorke (1979) and metric entropy (also known as Kolmogorov-Sinai entropy (Eckmann and Ruelle 1985)). The Lyapunov dimension is defined by  $D_L = k + \sum_{i=1}^k \lambda_i / |\lambda_{k+1}|$ , where  $k$  is the unique index such that  $\sum_{j=1}^k \lambda_j \geq 0$  and  $\sum_{i=1}^{k+1} \lambda_i < 0$ . Under general assumptions on the dynamical system under examination,  $D_L$  is an upper bound for the Hausdorff dimension of an attractor. The estimates for the dimension of an attractor obtained by computing the correlation and information dimensions (Farmer et al 1983) become completely meaningless when the Lyapunov dimension increases beyond, say, 20. In particular, the correlation and information algorithms tend to drastically underestimate the dimension. This is a well-known problem: for large dimensions, prohibitively long time series have to be used. Ruelle

(1990) suggests as a rule of thumb that a time series of  $10^d$  statistically independent data are needed in order to estimate an attractor of dimension  $d$ . Therefore, computational time and memory constraints in fact limit the applicability of correlation-like algorithms only to low-dimensional attractors.

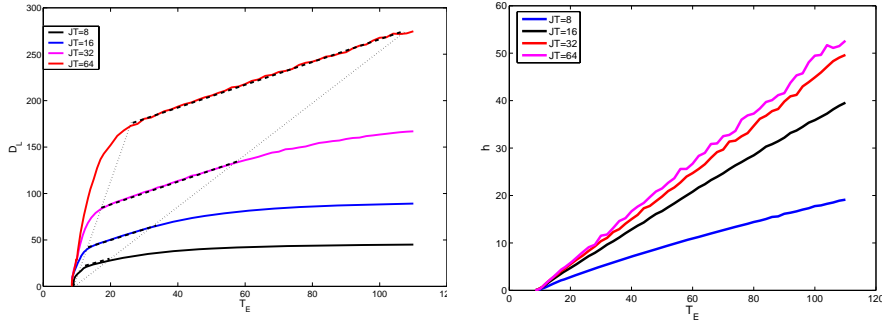


Fig. 1. Left: Lyapunov dimension of the attractor of the model as a function of  $T_E$ . All the straight lines are parallel and the domain of validity of the linear fit is apparently homothetic.

Right: metric entropy. Linear dependences  $h \approx \beta(T_E - T_E^{crit})$  occur for all values of  $JT$ .

The number of positive Lyapunov exponents - unstable dimension (Eckmann and Ruelle 1985) - increases with  $T_E$ , which implies that the Lyapunov dimension also does so. This is confirmed by a plot of the Lyapunov dimension as a function of  $T_E$  shown in Fig. 1 left. For small values of  $(T_E - T_E^{crit})$ , we have that  $D_L \propto (T_E - T_E^{crit})^\gamma$ , with  $\gamma$  ranging from  $\approx 0.5$  ( $JT = 8$ ) to  $\approx 0.7$  ( $JT = 64$ ). The range of  $T_E$  where this behavior can be detected increases with  $JT$ . For larger values of  $T_E$  a linear scaling regime of  $D_L \approx \eta T_E + const.$  is found in all cases. The linear coefficient is for all  $JT$  remarkably close to  $\eta \approx 1.2$ . The domain of validity of the linear approximation is apparently homothetic - see the simple geometric construction in Fig. 1 left. For  $T_E$  larger than a  $JT$ -depending threshold, there occurs a sort of phase-space saturation as the Lyapunov dimension begins to increase sublinearly with  $T_E$ . Note that while for  $JT = 8$  the model is in this regime in most of the explored  $T_E$ -domain ( $T_E \geq 20$ ), for  $JT = 64$  the threshold is reached only for  $T_E \geq 108$ . In this latter regime of parametric dependence the system is not able to provide an adequate representation of the details of the dynamics of the system.

The metric entropy  $h(\rho)$  of an ergodic invariant measure  $\rho$  expresses the mean rate of information creation, see Eckmann and Ruelle (1985) for definition and other properties. If a dynamical system possesses a SRB invariant measure  $\rho$ , then  $h(\rho)$  is equal to the sum of the positive Lyapunov exponents. Existence of an SRB measure is hard to prove for a given nonhyperbolic attractor. It has been only proven for

low-dimensional cases such as the Henon (Wang and Young 2001) or Lorenz (Viana 2000) strange attractors. We *assume* the existence of a *unique* SRB measure, coherently with the chaotic hypothesis proposed by Gallavotti and Cohen (1996; 1999), and refer to the sum of the positive Lyapunov exponents as metric entropy.

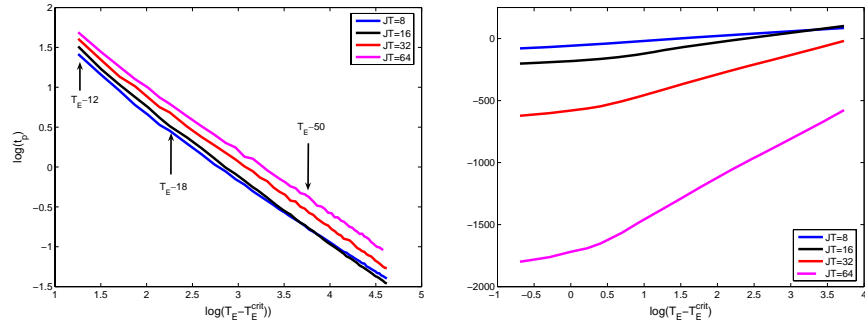


Fig. 2. Left: Log-Log plot of  $t_p = 1/\lambda_1$  versus  $T_E - T_E^{crit}$ . Right: Volume of the Bounding Box  $V_{BB}$  versus  $T_E - T_E^{crit}$ . For a description of the power-law fits, see text.

The mean predictability time for infinitesimal perturbations  $t_p = \lambda_1^{-1}$  as a function of  $T_E$  is plotted for  $JT = 8, 16, 32, 64$  in Fig. 2 left, while the metric entropy is presented in Fig. 1 right. It turns out that, for fixed  $JT$ ,  $\lambda_1$  increases sublinearly with  $T_E$ , whereas for  $T_E$  fixed,  $\lambda_1$  decreases for increasing values of  $JT$ . Consequently, for fixed  $JT$  the predictability time decreases monotonically with  $T_E$ . We note that, for all values of  $JT$ , if  $T_E > 14$  we have that  $t_p < 10$ , which corresponds in physical units to a predictability time  $t_p < 12$  days. Moreover, in the range  $T_E \geq 12$ ,  $t_p$  is proportional to  $(T_E - T_E^{crit})^\gamma$ , with  $\gamma$  ranging within  $[-0.85, -0.8]$  depending on the considered value of  $JT$ . The metric entropy has a marked linear dependence  $h \approx \beta(T_E - T_E^{crit})$ , with  $\beta$  ranging from  $\approx 0.15$  ( $JT = 8$ ) to  $\approx 0.5$  ( $JT = 64$ ). Moreover, for a given value of  $T_E$ , the metric entropy increases with  $JT$ . From the dynamical viewpoint, this means on one hand that the maximal sensitivity of the system to variations in the initial condition along a *single direction* is largest for  $JT = 8$ . On the other hand, there are more *active degrees of freedom* for  $JT = 64$  and they collectively produce a faster *forgetting* of the initial condition with time.

A more precise assessment of the time scales of the system and of predictability fluctuations may be gained by computing generalized Lyapunov exponents and performing the related multifractal diagnostics (Benzi et al. 1985, Paladin and Vulpiani 1987, Crisanti et al. 1993), which is outside the scope of this work.

### 3.2 Bounding Box of the Attractor

The bounding box of a set of points in an  $N$ -dimensional space is defined as the smallest hyperparallelepiped containing the considered set (Smith 2000). When the Hadley equilibrium is the attractor, the volume  $V_{BB} = 0$ , while it is non-zero if the computed orbit is attracted to a periodic orbit, a two-torus or a strange attractor. In all cases  $V_{BB}$ , which measures the bulk size of the attractor in phase space, grows with  $T_E$ . Actually, each of the factors in the product increases with  $T_E$ , so that expansion occurs in all directions of the phase space. This matches the expectations on the behavior of a dissipative system having a larger input of energy.

In the right panel of Fig. 2 we present a plot of  $\log(V_{BB})$  as function of  $T_E$  for the selected values of  $JT = 8, 16, 32$ , and  $64$ . In the case  $JT = 8$ ,  $V_{BB}$  obeys with great precision the power-law  $V_{BB} \propto (T_E - T_E^{crit})^\gamma$  in the whole domain  $T_E \geq 9$ . The best estimate for the exponent is  $\gamma \sim 40$ . Given that the total number of Fourier components is  $6 \times JT = 48$ , this implies that the growth of the each side of the bounding box is on the average proportional to about the  $5/6^{th}$  power of  $(T_E - T_E^{crit})$ . For  $JT \geq 16$ , two distinct and well defined power-law regimes occur:

$$V_{BB} \propto (T_E - T_E^{crit})^\gamma, \quad \gamma = \varepsilon N \quad \varepsilon \sim \begin{cases} 1/3, & T_E - T_E^{crit} \leq 1.5, \\ 5/6, & T_E - T_E^{crit} \geq 1.5, \end{cases} \quad (8)$$

where  $N = 6 \times JT$  is the number degrees of freedom. We emphasize that in all cases the uncertainties on  $\gamma$ , which have been evaluated with a standard bootstrap technique, are rather low and total to less than 3% of the best estimate of  $\gamma$ . Moreover, the uncertainty of the power-law fit greatly worsens if we detune the value of  $T_E^{crit}$  by, say, 0.3, thus reinforcing the idea that it is meaningful to fit a power-law against the logarithm of  $(T_E - T_E^{crit})$ .

The proportionality between the exponent and the number of degrees of freedom suggests considering separately the various sides of the bounding box hyperparallelepiped, *i.e.*, each of the factors in the product. For all values of  $JT$ , each side increases as  $(T_E - T_E^{crit})^{\gamma/N}$ , so that the hyperparallelepiped obeys a sort of self-similar scaling with  $T_E$ .

The comparison for various values of  $JT$  of factors in corresponding to the same spectral component for the same value of  $T_E - T_E^{crit}$  provides insight about the sensitivity to model resolution. The factors related to the the gravest latitudinal modes, such as agree with high precision, thus suggesting that the large scale behavior of the system is only slightly affected by variation of model resolution. When considering the terms related to the fastest latitudinally varying modes allowed by the lower resolution model, those obtained for  $JT = 32$  are *larger* than the corresponding factors obtained for  $JT = 64$ . This is likely to be the effect of spectral aliasing: the dynamics contained in the scales which are resolved in the higher-resolution models are projected in the fastest modes of the model with lower resolution.

## 4 Statistics of the total energy and zonal wind

### 4.1 Total energy

The total energy of the system  $E(t)$  is a global observable of obvious physical significance, statistically obeying a balance between the external forcing and the internal and surface dissipation. The horizontal energy density of the two-layer QG system can be expressed as follows:

$$e(x, y, t) = \frac{\bar{\delta}p}{g} \left[ \left( \bar{\nabla} \phi \right)^2 + \left( \bar{\nabla} \tau \right)^2 + \frac{2}{H_2^2} \tau^2 \right]. \quad (9)$$

Here the factor  $\bar{\delta}p/g$  is the mass per unit surface in each layer, the last term and the first two terms inside the brackets represent the potential and kinetic energy, respectively, thus featuring a clear similarity with the functional form of the energy of a harmonic oscillator. Note that in Eq. (10) the potential energy term is half of what reported in Pedlosky (1987), which contains a trivial mistake in the derivation of the energy density, as discussed with the author of the book. We consider as observable the total energy  $E(t)$ , evaluated by integrating the energy density expression:

$$E(t) = \int_0^{L_y} \int_0^{L_x} e(x, y, t) dx dy = 6 \int_0^{L_y} \int_0^{2\pi} e(x, y, t) dx dy. \quad (10)$$

Potential energy is injected into the system by zonally symmetric baroclinic forcing  $\tau^*$ . Part of it is transformed into wave kinetic energy by baroclinic conversion, and kinetic energy is eventually dissipated by friction such as that determined by Ekman pumping. This constitutes the Lorenz energy cycle (Lorenz 1955), which has been analyzed for this system in Speranza and Malguzzi (1988). In Tab. 1 we report the conversion factor of the total energy between the non-dimensional and dimensional units. For the Hadley equilibrium, the time-independent expression for the total energy is:

$$\overline{E(t)} = \frac{\bar{\delta}p}{g} L_x L_y \left( \frac{RT_E}{4f_0} \frac{1}{1 + \frac{\kappa}{v_E} \left( \frac{\pi}{L_y} \right)^2} \right)^2 \left( \frac{\pi^2}{L_y^2} + \frac{1}{H_2^2} \right). \quad (11)$$

The total energy is proportional to  $T_E^2$  and is mostly (95%) stored as potential energy, which is described by the second term of the sum in Eq. (11). In Fig. 3 we present the results obtained for the various values of  $JT$  used in this work. In the left panel we present the  $JT = 64$  case, which is representative of what obtained also in the other cases. The time-averaged total energy is monotonically increasing with  $T_E$ , but when the system enters the chaotic regime,  $\overline{E(t)}$  is much lower than the value for the coexisting Hadley equilibrium. This behavior may be related to the much larger dissipation fueled by the activation of the smaller scales. In the chaotic regime  $E(t)$  is characterized by temporal variability, which becomes more and more pro-

nounced for larger values of  $T_E$ . The overall agreement among the results obtained for  $\overline{E(t)}$  by choosing various  $JT$  values is good but progressively worsens when decreasing  $JT$ : for  $JT = 32$ , the maximal fractional difference is less than 0.01, while for  $JT = 8$  it is about one order of magnitude larger. Differences among the representations given by the various truncations levels also emerge in power-law fits such as  $\overline{E(t)} \propto T_E^\gamma$ . In the regime where the Hadley equilibrium is attracting, this fit is exact, with exponent  $\gamma = 2$ . For  $T_E - T_E^{crit} \leq 1.5$  and  $T_E > T_E^H$  (the value of the first Hopf bifurcation, see Tab. 3), for all the values of  $JT$  the power-law fit is good, with  $\gamma = 1.90 \pm 0.03$ , so that a weakly subquadratic growth is realized. For  $T_E - T_E^{crit} \geq 1.5$ , only the  $JT = 32$  and 64 simulations of  $\overline{E(t)}$  obey with excellent approximation a weaker power-law, with  $\gamma = 1.52 \pm 0.02$  in both cases, while the cases  $JT = 8$  and 16 do not satisfactorily fit any power-law. The agreement worsens in the upper range of  $T_E$ , which points at the criticality of the truncation level when strong forcings are imposed. Nevertheless, the observed differences are strikingly small between the cases, say,  $JT = 8$  and  $JT = 64$ , with respect to what could be guessed by looking at the Lyapunov dimension, entropy production, and bounding box volume diagnostics analyzed in the previous sections.

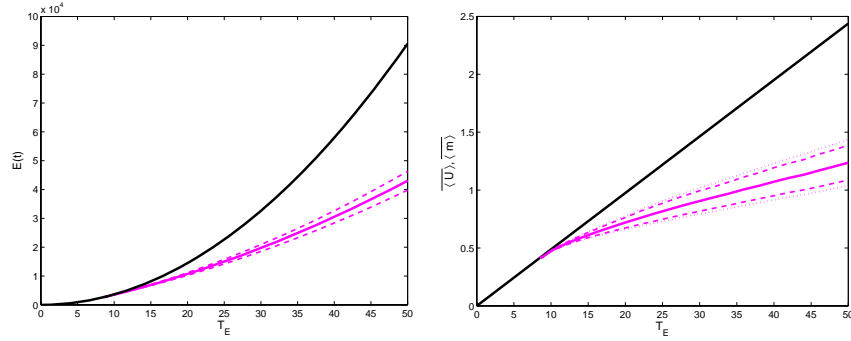


Fig. 3. Left:  $\overline{E(t)}$  obtained from model integrations for  $JT = 64$  (magenta line) and for Hadley equilibrium (black line). Right:  $\langle \overline{U(t)} \rangle = \langle \overline{m(t)} \rangle$  obtained from model integrations for  $JT = 64$  (magenta line) and for Hadley equilibrium (black line). See text for details.

## 4.2 Zonal wind

We consider  $U(y, t) = 1/2(u_1(y, t) + u_3(y, t))$  and  $m(y, t) = 1/2(u_1(y, t) - u_3(y, t))$ , which represent the zonal average of the mean and of the halved difference of the zonal wind at  $p = p_1$  and  $p = p_3$  at latitude  $y$ , respectively. The latitudinal average  $\langle U(y, t) \rangle$  is then proportional to the total zonal momentum of the atmosphere,

whereas  $\langle m(y, t) \rangle$ , by geostrophic balance, is proportional to the equator-to-pole temperature difference. Computation of the latitudinal average at the time-independent Hadley equilibrium is straightforward:

$$\langle m(y) \rangle = \langle U(y) \rangle = \frac{R}{f_0 L_y} \frac{T_E}{2} \frac{1}{1 + \frac{\kappa}{v_N} \left( \frac{\pi}{L_y} \right)^2}. \quad (12)$$

Since we cannot have net, long-term zonal forces acting on the atmosphere at the surface interface, the spatial average of the zonal wind at the  $p = p_3$  must be zero. Therefore, the outputs of the numerical integrations must satisfy the constraint  $\langle m(y, t) \rangle = \langle U(y, t) \rangle$ , where  $\bar{X}$  denotes the time-average of the field  $X$ . In the right panel of Fig. 3 we plot the outputs for  $JT = 64$ , which, similarly to the total energy case, is well representative of all the  $JT$  cases. The constraint is obeyed within numerical precision. The average winds are monotonically increasing with  $T_E$ , but, when the system enters the chaotic regimes, the averages  $\langle m(y, t) \rangle = \langle U(y, t) \rangle$  have a smaller value than at the corresponding Hadley equilibrium, and they display sublinear growth with  $T_E$ . Moreover, for  $T_E > T_E^{crit}$  the temporal variability of the time series  $\langle m(y, t) \rangle$  and  $\langle U(y, t) \rangle$  increases with  $T_E$ . The variability of  $\langle m(y, t) \rangle$  is larger than that of  $\langle U(y, t) \rangle$ , probably because the latter is related to a *bulk* property of the system such as the total zonal momentum.

The overall agreement between the various truncation levels progressively worsens for smaller  $JT$ , similarly to what observed for the total energy of the system. In particular, differences emerge as one attempts power-law fits of the form  $\langle m(y, t) \rangle = \langle U(y, t) \rangle \propto T_E^\gamma$ . For the Hadley equilibrium regime we have  $\gamma = 1$ . For  $T_E \leq 10$  and above the first Hopf bifurcation, for all values of  $JT$  the power-law fit is good, with  $\gamma = 0.875 \pm 0.005$ . For  $T_E - T_E^{crit} \geq 1.5$ , only the simulations with  $JT = 32$  and 64 obey a power-law (with  $\gamma = 0.58 \pm 0.02$ ) with excellent approximation.

This implies that while the time-averaged meridional temperature difference between the northern and southern boundary of the system increases monotonically with  $T_E$ , as to be expected, the realized value is greatly reduced by the onset of the chaotic regime with respect to the corresponding Hadley equilibrium. This is the signature of the negative feedback due to the following mechanism: when the poleward eddy transport of heat is realized, it causes the reduction of the meridional temperature gradient, thus limiting by geostrophy the wind shear, which causes in turn a reduction of baroclinically-induced eddies *towards* the marginal stability. This process can be considered to be the statistical generalization of the classical *baroclinic adjustment* (Stone 1978). The latter implies that the system balances near an average state which corresponds to a fixed point which is neutral with respect to baroclinic instability. Theoretical justifications for this type of adjustment often rely on the idea that a variational principle holds for the relationship between the basic state gradient and the heat and momentum fluxes. This is the case, *e.g.*, of classical



convection, for which it can be proved that the most unstable mode is the one carrying heat most efficiently in the direction of the basic state gradient. In fact, such a variational principle does not hold for ordinary baroclinic instability, as it can be proved that the most rapidly growing baroclinic mode is not the one with the largest heat flux. But in this model, as opposed to the general case, the variational assumption in question is essentially correct, since only one zonal wave is considered (Speranza and Malguzzi 1988). Nevertheless, the adjustment mechanism does not keep the system *close to marginal stability* since for  $T_E > T_E^{crit}$  both the instantaneous and the time-averaged fields of the system are rather different from those realized for  $T_E \approx T_E^H$ , near the edge of the Hadley equilibrium. This denies the possibility that the time-mean circulation is maintained by eddies which can be parameterized in terms of the time-mean fields.

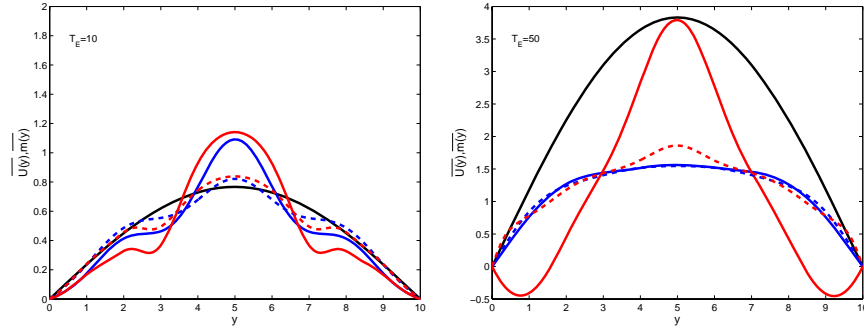


Fig. 4. Time-averaged profiles  $\overline{U}(y)$  (solid lines) and  $\overline{m}(y)$  (dashed lines). The black line indicates the  $U(y) = m(y)$  Hadley equilibrium profiles. Red (blue) line refers to the  $JT = 8$  ( $JT = 32$ ) case.  $T_E$  is indicated. Vertical scale on the left figure is 1/2 of that of the right figure.

By examining more detailed diagnostics on the winds, such as the time-averaged latitudinal profiles of  $U(y)$  and of  $m(y)$  (Fig. 4), relevant differences are observed between  $JT = 8$  and the other three cases. Results are presented for  $JT = 8$  and  $JT = 32$ , the latter being representative also of  $JT = 16$  and  $64$ . We first note that already for  $T_E = 10$ , such that only a weakly chaotic motion is realized, the  $U(y)$  and  $m(y)$  profiles feature in both resolutions relevant qualitative differences with respect to the corresponding Hadley equilibrium profile, although symmetry with respect to the center of the channel is obeyed. The  $\overline{U}(y)$  and  $\overline{m}(y)$  profiles are different (the constraint being still satisfied), with  $\overline{U}(y) > \overline{m}(y)$  at the center and  $\overline{U}(y) < \overline{m}(y)$  at the boundaries of the channel. Nevertheless, like for the Hadley equilibrium, both  $\overline{U}(y)$  and  $\overline{m}(y)$  are positive and are larger at the center of the channel than at the boundaries. Consequently, at  $p = p_1$  there is a westerly flow at the center of the

channel and easterly flows at the two boundaries. At  $p = p_3$  the wind is everywhere westerly and peaks at the center of the channel. Such features are more pronounced for the  $JT = 32$  case, where the mechanism of the convergence of zonal momentum is more accurately represented.

For larger values of  $T_E$ , the differences between the two truncation levels become more apparent. For  $JT = 8$ , the observed  $\overline{U}(y)$  and  $\overline{m}(y)$  profiles tend to flatten in the center of the channel and to become more similar to each other. Therefore, somewhat similarly to the Hadley equilibrium case, the winds at  $p = p_1$  tend to vanish and all the dynamics is restricted to  $p = p_3$ . The  $\overline{m}(y)$  profiles for  $JT = 32$  are quite similar to those of  $JT = 8$ , even if they peak and reach higher values in the center of the channel and are somewhat smaller at the boundaries. So when a finer resolution is used, a stronger temperature gradient is realized in the channel center. The  $\overline{U}(y)$  profiles obtained for  $JT = 32$  are instead very different. They feature a strong, well-defined peak in the channel center and negative values near the boundaries. Therefore, the winds in the upper pressure level are strong westerlies, and peak in the center of the channel, while the winds in the lower pressure level feature a relatively strong westerly jet in the center of the channel and two compensating easterly jets at the boundaries. The fact that for higher resolution the wind profiles are less smooth and have more evident jet-like features is related to the more efficient mechanism of barotropic stabilization, which, through zonal wind convergence, *keeps the jet together* (Kuo 1973).

## 5 Summary, Conclusions and Future Developments

We have described the construction and the dynamical behavior of an *intermediate complexity* model of the atmospheric system. We take as prototypal model for the GAC a QG two-layer model where the mid-latitude atmosphere is taken as being composed of two-layers and the beta-plane approximation is considered.

A single zonal wave solution is assumed and by a spectral discretization in the latitudinal direction, the latter equation is reduced to a system of  $N=6 \times JT$  ordinary differential equations, where  $JT+1$  is the number of nodes of the (latitudinally speaking) fastest varying base function. We have considered the cases  $JT = 8, 16, 32$ , and 64. Although obviously relevant ingredients of geometrical (horizontal convergence due to the Earth curvature, latitudinal boundary conditions at the margins of the mid-latitudes, circumpolar vortex, etc.) and dynamical (stabilization mechanisms such as the so-called *barotropic governor* (Nakamura 1993) nature of the real atmospheric circulation are still missing in this simplified theoretical representation, the model features some fundamental processes determining the general circulation of the Earth atmosphere. In particular, the acting processes are the baroclinic conversion, trans-

forming available potential energy into waves; the nonlinear stabilization of the zonal jet by eddy momentum convergence from non-symmetric disturbances; and the thermal diffusion and Ekman pumping-driven viscous dissipation.

When a larger pool of available energy is provided, the dynamics of the system is richer, since the baroclinic conversion process can transfer larger amounts of energy to the disturbances. Correspondingly, by increasing the parameter  $T_E$ , which parameterizes the baroclinic forcing, the overall behavior of the system is greatly altered. The attractor changes from a fixed point to a strange attractor via a finite number of bifurcations, starting with a Hopf bifurcation at  $T_E = T_E^H$  determining the loss of stability of the Hadley equilibrium, and a final two-torus breakdown at  $T_E = T_E^{crit}$ .

The strange attractor is studied by means of the Lyapunov exponents. The Lyapunov spectra obtained for  $JT = 32, 64$  resemble what obtained in more complex QG models (Vannitsem 1997; Snyder and Hamill 2003). A striking feature of this dynamical system is the smooth dependence on  $T_E$  of all of its dynamical properties. The metric entropy, representing the overall total dynamical instability, increases linearly with  $T_E$  for  $T_E > T_E^{crit}$  for all examined values of  $JT$ , and is increases with  $JT$ . The Lyapunov dimension  $D_L$  increases with both  $T_E$  and  $JT$ . In particular, by increasing  $T_E$ , initially the dimension grows with a sublinear power-law  $D_L \propto (T_E - T_E^{crit})^\gamma$ , followed by a linear scaling regime, while for large  $T_E$ ,  $D_L$  saturates. The fact that the dimensionality of the attractor increases with the total energy of the system (they are both monotonically increasing with  $T_E$ ) suggest that the system has a positive temperature, in a statistical mechanical sense. For  $JT \geq 16$ , each side of the bounding box of the attractor increases as  $\propto (T_E - T_E^{crit})^{1/3}$  for  $T_E - T_E^{crit} \leq 1.5$  and as  $\propto (T_E - T_E^{crit})^{5/6}$  for larger values of  $T_E$ , while for  $JT = 8$  only the latter regime is present. Therefore, the ratios of the ranges of the various degrees of freedom remain essentially unchanged when varying  $T_E$ , yielding a self-similar scaling property.

When the system enters the chaotic regime, the average total energy and average zonal winds have lower values than those of the corresponding unstable Hadley equilibrium, because the occupation of the faster-varying latitudinal modes fuels Ekman pumping-driven viscous dissipation, which acts preferentially on the small scales. The total energy and the average wind field obey with excellent approximation a subquadratic and sublinear power-laws  $\propto T_E^\gamma$ , respectively, and are in *quantitative* agreement for all values of  $JT$ , essentially because these quantities are representative of global balances.

If general enough, the scaling properties could be of great help in setting up a theory for the overall statistical properties of the GAC and in guiding - on a heuristic basis - both data analysis and realistic simulations. A leading example for this would be the possibility of estimating the sensitivity of the output of the system with respect to changes in the parameters. Physical insight into the relevant mechanisms can

be obtained by considering the main feedback mechanisms setting the average statistical properties of the system, *e.g.* when changing the forcing  $T_E$  from  $T_E = T_E^0 > T_E^{crit}$  to  $T_E = T_E^0 + \Delta T_E$ . The change in  $T_E$  directly causes an increase in the wind shear through Newtonian forcing and indirectly an increase in the value of the mean zonal momentum through Ekman pumping. The increase in the wind shear enhances the baroclinic conversion and so the eddy components. In turn, the eddy stresses act as feedback by depleting baroclinity and by increasing the momentum through barotropic convergence, which closes the feedback loop. In the chaotic regime, these feedback mechanisms act as a statistical baroclinic adjustment process, which reduces the average value of the equator-to-pole temperature difference. This process is not reducible to the stationary balances of the classical theory of GAC, since it takes place when the system lives in a strange attractor. This situation certainly corresponds more closely, at least at the conceptual level, to the equilibration occurring in the atmosphere. Preliminary calculations performed by the authors together with Vannitsem (unpublished results) suggest that the power-laws presented here hold also on simplified yet global models of the atmospheric circulation, so the obtained scalings laws might be very helpful in establishing a sort of bulk *climate theory* for the atmospheric disturbances.

The fact that all the considered dynamical indicators and physical quantities feature a smooth, simple dependence with respect to the forcing parameter  $T_E$  and a limited variation is at first striking if one keeps in mind the phenomena typically occurring in low-dimensional systems. The latter often feature *attractor crises*, which are bifurcations in which the size and shape of a strange attractor drastically changes across a suitable parameter value (see Robert et al. (2000) and references therein). A particular type of crisis occurs when a saddle-node bifurcation takes place on the strange attractor, which is destroyed, and an attracting equilibrium or periodic orbit is created. This *phase-locked* attractor persists for an interval - *window of periodicity* - of parameter values, outside of which the strange attractor reappears. Such windows of periodicity are known to occur in many systems and are even dense in the parameter space of certain one-dimensional models (Broer et al. 2002). Although bifurcations certainly occur as  $T_E$  varies in the fully chaotic regime (*e.g.*, at the values where a Lyapunov exponent crosses zero and becomes positive), these bifurcations do not induce sharp variations or crises. Moreover, we strongly doubt that there is a way to explain the smooth behaviour of the system by relating it to the bifurcation where the strange attractor is created, since the latter occurs for much lower values of  $T_E$ . Also compare the discussion in Speranza and Malguzzi (1988)

Moreover, when beyond a certain threshold of a parameter new physical processes come into play or a given process reaches a qualitatively distinct statistical balance, we do not expect to find a global uniform parametrically-controlled self-scaling of the system statistical properties. The change in the slope observed for

value of  $T_E - T_E^{crit} \approx 1.5$  may then be interpreted as a somewhat fundamental changeover from a quasi-linear baroclinic activity to a fully chaotic regime. A possible source of large - anyway likely to be smooth - and non-self-similar variations of the statistical properties of the attractor with respect to external parameters is resonant behavior, *i.e.* the preferential occurrence of certain physical processes for a bounded range of values of a given parameter. In the case of atmospheric dynamics, this effect might be more relevant than the occurrence of windows of periodicity, although in a range of variability which is different from what explored here, namely the low-frequency variability (Malguzzi and Speranza 1981; Benzi et al. 1986; Benzi and Speranza 1989; Ruti et al. 2006).

The chaotic hypothesis (Gallavotti and Cohen 1996; 1999) and the conjectures in (Albers and Sproot 2006) express similar concepts: despite the fact that the available theoretical and phenomenological evidence indicates that structural stability of systems having strange attractors is not typical, from the physical/numerical point of view typical chaotic systems behave *as though* they were structurally stable under perturbations if the dimension is sufficiently high. This fundamental assertion has both diagnostic and prognostic consequences: from the diagnostic viewpoint, the conjectures in (Albers and Sproot 2006) state that systems of the considered type display smooth-like dependence on external parameters; from the prognostic viewpoint, the chaotic hypothesis allows establishing fluctuation-dissipation theorems and Onsager relations in certain models for developed turbulence (Gallavotti and Cohen 1999). We propose that the windows of periodicity, if existing at all, are so narrow to be not detectable, and that the SRB measure varies continuously on the parameter set where a strange attractor exists.

An interesting approach is understanding the statistical properties of the waves as a function of the zonal wind fields, taken, as a first approximation, as external stochastic inputs with given statistical properties parameterized in terms of  $T_E$ . This amounts to considering the zonal wind as a sort of integrator of the wave disturbances, which is consistent with the almost-linearity of the evolution equations of the wave components of the model considered in this study. Such a framework, which assumes the possibility of neglecting the direct wave-wave interactions, seems to be well justified (Schneider 2006). The evolution equations for the wave fields, indicated as  $\vec{x}$ , can be represented to be of the form  $\dot{\vec{x}} = M(t)\vec{x}$ , where  $M$  is a random square matrix (Crisanti et al. 1993) whose statistical properties depend on those of the  $U$  and  $m$  fields. Therefore, the study of the statistics of  $M$ , *e.g.* eigenvalues, eigenvectors, singular values, singular vectors, as a function of  $T_E$  may inform us on the properties of the generated waves, which can be associated to the destabilizing and stabilizing physical processes. The acknowledgement of the inadequacy of the paradigm of neutral atmospheric waves and of the need of a detailed description of the statistics of growth and decay of the waves would have far-reaching impacts. In

fact, when considering the spectral representation of the mid-latitude waves of the real or *realistic* (i.e. resulting from models such as GCMs) atmosphere, we find 2D wavenumber-frequency spectral densities that only vaguely correspond, in a statistical sense, to well-defined dispersion relations  $\omega = \omega(k)$ , since at all frequencies the spectral width is relatively wide, essentially because of the finite life cycle of the waves (Dell'Aquila et al. 2005; Lucarini et al. 2006). Moreover, such a random-matrix approach might serve also to understand at mathematical level the power-law scalings and thus making a sense of the self-similarity of the system's properties. Note that due to the absence of direct wave-wave interactions, this approach is somewhat dual with respect to a turbulence-oriented approach.

Further main, necessary directions of future work along the proposed line of approach to GAC can be summarized as follows:

- Analyzing the debated properties in more articulated numerical models. An important issue may be the separation of the properties of the baroclinic mid-latitude jet system from the low-frequency variability; using more realistic atmospheric models comprising bottom orography, a physically interesting experiment to be performed with the purpose of finding the break-up of self-similarity is to parameterically tune and detune the onset of the orographic baroclinic energy conversion (Buzzi et al. 1984, Ruti et al. 2006).
- Consolidating and explaining the knowledge - see Schneider (2006) - that in the real atmosphere the dynamics of traveling baroclinic disturbances is dominated by the *wave-zonal flow* interaction and the role of the *wave-wave* interaction is minor. This may be crucial for modeling in detail the extratropical storm tracks (Hoskins and Valdes 1990).

## References

- D. J. Albers, J. C. Sprott: Structural stability and hyperbolicity violation in high-dimensional dynamical systems, *Nonlinearity* **19** (2006), 1801–1847.
- R. Benzi, G. Paladin, G. Parisi, A. Vulpiani: Characterisation of intermittency in chaotic systems. *J. Phys. A* **18** (1985), 2157–2165.
- R. Benzi, P. Malguzzi, A. Speranza, A. Sutera: The statistical properties of general atmospheric circulation: observational evidence and a minimal theory of bimodality. *Quart. J. Roy. Met. Soc.* **112** (1986), 661–674.
- R. Benzi, A. Speranza: Statistical properties of low frequency variability in the Northern Hemisphere. *J. Climate* **2** (1989), 367–379.
- C. Bonatto, J. C. Garreau, J.A.C. Gallas: Self-similarities in the frequency-amplitude space of a loss-modulated CO<sub>2</sub> laser, *Phys. Rev. Lett.* **95** 143905 (2005).

- H.W. Broer, C. Simó, R. Vitolo: Bifurcations and strange attractors in the Lorenz-84 climate model with seasonal forcing, *Nonlinearity* **15** (2002), 1205–1267.
- A. Buzzi, A. Trevisan, A. Speranza: Instabilities of a baroclinic flow related to topographic forcing, *J. Atmos. Sci.* **41** (1984), 637–650.
- J.G. Charney: The Dynamics of Long Waves in a Baroclinic Westerly Current, *J. Atmos. Sci.* **4** (1947), 136–162.
- J.G. Charney: On the scale of atmospheric motions. *Geofys. Publik.* **17** (1948), 251–265.
- J.G. Charney, J.C. Devore: Multiple flow equilibria in the atmosphere and blocking. *J. Atmos. Sci.* **36** (1979), 1205–1216.
- E.G.D. Cohen and G. Gallavotti: Note on Two Theorems in Nonequilibrium Statistical Mechanics, *J. Stat. Phys.* **96** (1999), 1343–1349.
- A. Crisanti, G. Paladin and A. Vulpiani: *Products of Random Matrices in Statistical Physics*, Springer, New York, 1993.
- E.T. Eady: Long waves and cyclone waves, *Tellus* **1** (1949), 33–52.
- J.-P. Eckmann, D. Ruelle: Ergodic theory of chaos and strange attractors, *Rev. Mod. Phys.* **57** (1985), 617–655.
- A. Dell’Aquila, V. Lucarini, P.M. Ruti, S. Calmanti: Hayashi spectra of the northern hemisphere mid-latitude atmospheric variability in the NCEP–NCAR and ECMWF reanalyses, *Clim. Dyn.* **25** (2005), 639–652.
- H. A. Dijkstra: *Nonlinear Physical Oceanography*, Springer, New York, 2005.
- J.D. Farmer: Chaotic attractors of an infinite-dimensional dynamic system, *Physica D* **4** (1982), 366–393.
- J.D. Farmer, E. Ott, and J.A. Yorke: The dimension of chaotic attractors, *Physica D* **7** (1983), 153–180.
- M. Felici, V. Lucarini, A. Speranza, R. Vitolo: Extreme Value Statistics of the Total Energy in an Intermediate Complexity Model of the Mid-latitude Atmospheric Jet. Part I: Stationary case, *J. Atmos. Sci.*, in press (2006)
- C. Foias, E.J. Olson: Finite Fractal Dimension and Holder-Lipschitz Parametrization, *Indiana Uni. Math. J.* **45** (1996), 603–616
- P.K. Friz, J.C. Robinson: Parametrising the attractor of the two-dimensional Navier–Stokes equations with a finite number of nodal values, *Physica D* **148** (2001), 201–220
- G. Gallavotti: Chaotic hypothesis: Onsager reciprocity and fluctuation-dissipation theorem, *J. Stat. Phys.* **84** (1996), 899–926.
- M. Ghil, R. Benzi, G. Parisi (Eds.), *Turbulence and Predictability in Geophysical Fluid Dynamics and Climate Dynamics*, North-Holland, Amsterdam, 1985.
- D. Schertzer, S. Lovejoy: Uncertainty and Predictability in Geophysics: Chaos and Multifractal Insights in *The State of the Planet: Frontiers and Challenges in Geophysics*, American Geophysical Union, Washington, 2004.
- I.M. Held: The Gap between Simulation and Understanding in Climate Modeling, *Bull. Am. Meteor. Soc.* (2005), 1609–1614.

- I.M. Held, A.Y. Hou: Nonlinear Axially Symmetric Circulations in a Nearly Inviscid Atmosphere, *J. Atmos. Sci.* **37** (1980), 515–533
- M. Hénon, Y. Pomeau: Two strange attractors with a simple structure, in *Turbulence and Navier-Stokes equations* **565** (1976), Springer-Verlag, 29–68.
- B.J. Hoskins, P.J. Valdes: On the existence of storm-tracks, *J. Atmos. Sci.* **47** (1990), 1854–1864.
- E. Kalnay: Atmospheric modeling, data assimilation and predictability, Cambridge Univ. Press, Cambridge, 2003.
- J. Kaplan, J. Yorke: Chaotic behaviour of multidimensional difference equations, in *Functional Differential Equations and Approximations of Fixed Points, Springer LNM* (1979), 204–227.
- R. Kubo: The Fluctuation Dissipation Theorem, *Rep. Prog. Phys.* **29** (1966), 255–284.
- H.L. Kuo: Dynamics of quasigeostrophic flows and instability theory, *Adv. Appl. Mech.* **13** (1973), 247–330.
- C.E. Leith: Climate response and fluctuation dissipation, *J. Atmos. Sci.* **32** (1975), 2022–2026.
- E.N. Lorenz: Available potential energy and the maintenance of the general circulation, *Tellus* **7**, (1955), 157–167.
- E.N. Lorenz: The Nature and Theory of the General Circulation of the Atmosphere, World Meteorol. Organ., Geneva, 1967.
- E.N. Lorenz: The predictability of a flow which possesses many scales of motion, *Tellus* **21**, (1969), 289–307.
- E.N. Lorenz: Forced and Free Variations of Weather and Climate, *J. Atmos. Sci.* **36** (1979), 1367–1376.
- E.N. Lorenz: Attractor sets and quasi-geostrophic equilibrium, *J. Atmos. Sci.* **37** (1980), 1685–1699.
- V. Lucarini: Towards a definition of climate science, *Int. J. Environ. Pollut.* **18** (2002), 409–414.
- V. Lucarini, J.J. Saarinen, K.-E. Peiponen, E. Vartiainen: *Kramers-Kronig Relations in Optical Materials Research*, Springer, Heidelberg, 2005.
- V. Lucarini, S. Calmanti, A. dell’Aquila, P.M. Ruti, A. Speranza: Intercomparison of the northern hemisphere winter mid-latitude atmospheric variability of the IPCC models, *Clim. Dyn.* DOI: 10.1007/s00382-006-0213-x (2006)
- P. Malguzzi, A. Speranza: Local Multiple Equilibria and Regional Atmospheric Blocking, *J. Atmos. Sci.* **9**, 1939–1948.
- P. Malguzzi, A. Trevisan, A. Speranza: Statistics and predictability for an intermediate dimensionality model of the baroclinic jet, *Ann. Geoph.* **8** (1990), 29–35.
- R. Mantovani, A. Speranza: Baroclinic instability of a symmetric, rotating, stratified flow: a study of the nonlinear stabilisation mechanisms in the presence of viscosity, *Nonlinear Processes in Geophysics* **9** (2002), 487–496.
- M. Margules: Die energie der Stürme. *Jahrb. Zentralanst. Meteor. Wien*, **40** (1903), 1–26.



- N. Nakamura: Momentum flux, flow symmetry, and the nonlinear barotropic governor, *J. Atmos. Sci.* **50** (1993), 2159–2179.
- V.I. Oseledec: A multiplicative ergodic theorem. Lyapunov characteristic numbers for dynamical systems, *Trudy Mosk. Mat. Obsc. (Moscow Math. Soc.)* **19** (1968), 19.
- G. Paladin, A. Vulpiani: Anomalous scaling laws in multifractal object. *Phys. Rep.* **156** (1987), 147–225.
- J. Pedlosky: *Geophysical Fluid Dynamics*. 2nd ed., Springer-Verlag, 1987.
- N.A. Phillips: Energy transformations and meridional circulations associated with simple baroclinic waves in a two-level, quasi-geostrophic model, *Tellus* **6** (1954), 273–286.
- A. Randriamampianina, W.-G. Früh, P. Maubert, P.L. Read: DNS of bifurcations to low-dimensional chaos in an air-filled rotating baroclinic annulus, *preprint at* <http://www-atm.physics.ox.ac.uk/user/read/> (2005).
- C. Robert, K. T. Alligood, E. Ott, J. A. Yorke: Explosions of chaotic sets, *Physica D: Nonlinear Phenomena*, **144(1-2)** (2000), 44–61.
- D. Ruelle: Deterministic chaos: the science and the fiction, *Proc. R. Soc. London A* **427** (1990), 241–248.
- P.M. Ruti, V. Lucarini, A. Dell’Aquila, S. Calmanti, A. Speranza: Does the subtropical jet catalyze the mid-latitude atmospheric regimes? , *Geophys. Res. Lett.* **33**: L06814 (2006).
- T. Schneider: The general circulation of the atmosphere, *Ann. Rev. Earth Plan. Sci* **34** (2006) 655–688, DOI:10.1146/annurev.earth.34.031405.125144.
- L.A. Smith: Disentangling Uncertainty and Error: On the Predictability of Nonlinear Systems, in *Nonlinear Dynamics and Statistics*, A. Mees ed., Birkhauser, Boston (2000) 31–64.
- C. Snyder, T.M. Hamill: Leading Lyapunov vectors of a turbulent baroclinic jet in a quasi-geostrophic model, *J. Atmos. Sci.* **60** (2003), 683–688
- A. Speranza, V. Lucarini: Environmental Science: physical principles and applications, in *Encyclopedia of Condensed Matter Physics*, F. Bassani, J. Liedl, P. Wyder eds., Elsevier, Amsterdam, in press (2005).
- A. Speranza, P. Malguzzi: The statistical properties of a zonal jet in a baroclinic atmosphere: a semilinear approach. Part I: two-layer model atmosphere, *J. Atmos. Sci.* **48** (1988), 3046–3061.
- P.H. Stone: Baroclinic adjustment, *J. Atmos. Sci.* **35** (1978), 561–571.
- S. Vannitsem, C. Nicolis: Lyapunov vectors and error growth patterns in a T21L3 quasi-geostrophic model, *J. Atmos. Sci.* **54** (1997), 347–361.
- M. Viana: What’s new on Lorenz strange attractors? , *Math. Intelligencer* **22-3** (2000), 6–19.
- Q. Wang, L.-S. Young: Strange Attractors with One Direction of Instability, *Comm. Math. Phys.* **218** (2001), 1–97